



Comparison of long-term radii evolution of the S-phase in aluminum alloy 2618A during ageing and creep

Christian Rockenhäuser^{a,*}, Sina Schriever^a, Philipp von Hartrott^b, Benjamin Piesker^a, Birgit Skrotzki^a

^a Bundesanstalt für Materialforschung und -prüfung (BAM), Experimental and Model Based Mechanical Behavior of Materials, Unter den Eichen 87, 12205 Berlin, Germany

^b Fraunhofer Institut für Werkstoffmechanik IWM, 79108 Freiburg, Germany

ARTICLE INFO

Keywords:

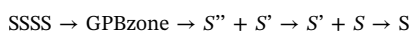
Aluminum alloys
Electron microscopy
Ageing
Creep
Microstructure
S-phase

ABSTRACT

A study was made on the effect of creep loading on the precipitate radii evolution of the aluminum alloy 2618A. The overageing process of the alloy was investigated under load at a temperature of 190 °C with stresses between 79 and 181 MPa and compared to stress free isothermal ageing. The precipitates responsible for strength were characterized using dark-field transmission electron microscopy (DFTEM). This allows the experimental determination of radii distributions of the rod-shaped Al₂CuMg precipitates and the evaluation regarding their mean precipitate radius. It was found that the mean precipitate radius enables the comparison of the different microstructural conditions of crept and uncrept samples. The mean precipitate radii of the samples experiencing creep are significantly higher than those of undeformed samples. It was shown that the acquired radii distributions are viable to determine averaged particle radii for comparison of the aged samples. A ripening process including pipe diffusion along dislocations describes the data on coarsening very well for the creep samples.

1. Introduction

The Al-Cu-Mg aluminum alloy 2618A is part of the 2XXX series of aluminum alloys, which is used in transportation and aerospace industry for long term operation at elevated temperature due to its desirable material properties (e.g. high creep resistance) [1]. It contains a certain amount of Fe and Ni to form intermetallic compounds of μm-size, which provide dispersion strengthening and retain microstructural stability at elevated temperatures [2–5]. The strength is mainly controlled by the distribution of the nm-sized secondary S-phase, which is formed from the supersaturated solid solution (SSSS) during heat treatments [6–10]. The equilibrium S-Phase is orthorhombic and has the composition Al₂CuMg [11,12]. The first decomposition sequence proposed was [13,14]:



The Guinier-Preston-Bagaryatski (GPB) zones were named by Silcock [13] and are rods of 1–2 nm in diameter. The S'' and S' were reported to be metastable variants of the S-phase. It was later suggested by Ringer et al. [15–17] that the GPB zones are preceded by Cu-Mg co-clusters. In general, the decomposition sequence of the rod-shaped hardening phases during isothermal ageing remains under debate

[18,19]. It was shown that the nucleation of the precipitates can be strongly affected by external stresses in different Al-alloy systems [20–23]. The first quantitative solution of the coarsening was proposed by Lifshitz and Slyozov [24] and Wagner [25] with

$$r^3 - r_0^3 = k(t - t_0) \quad (1)$$

where r is the mean radius, r_0 is the initial mean radius, t the coarsening time and t_0 the beginning of the coarsening process. However, the equation is only valid, if the following conditions are met: i) The mass transport needs to be isotropic, ii) the precipitates exhibit a statistical size distribution, iii) there is no local strain of the lattice during coarsening, and iv) the volume fraction of the secondary phase is small. In addition, a modification of the equation is necessary due to the rod-shaped morphology of the S-phase precipitates. Speich and Oriani derived the same power law as shown in Eq. (1), where k is modified by the aspect ratio of the precipitates [26]. Hence, as an additional condition, the aspect ratio of the precipitates needs to be constant. An experimental study of Monzen et al. confirmed this for α -Fe particles in a Cu matrix [27]. An external load may influence and change the coarsening process of the secondary phase due to several reasons. Strain in general influences the diffusion flux in material with homogeneous elemental distributions and can be described as a deviation from

* Corresponding author.

E-mail address: Christian.Rockenhaeuser@bam.de (C. Rockenhäuser).

Ficks' Laws [28]. In case of alloys containing precipitates, an external strain may also influence the growth of the precipitates due to changes in the interfacial equilibrium concentrations, hence altering relative stability of precipitate and matrix phases [29]. In addition, plastic deformation influences the precipitate coarsening. It is well-known that the mass transport along lattice defects like dislocations and grain boundaries may elapse faster [30]. Ardell proposed the following equation for precipitate coarsening with accelerated growth:

$$r^5 - r_0^5 = k(t - t_0) \quad (2)$$

This relationship is expected for precipitates which are connected by a dislocation network and the mass transport then elapsed with increased speed along dislocations as diffusion pathways [31].

In the present work, the microstructure evolution of peak aged samples of alloy 2618A was studied during thermal exposure. Ceschini et al. [32] reported that exposure at temperatures ≥ 200 °C results in a significant decrease of sample hardness. Their microstructural investigations showed that the hardness decrease over time coincides with a coarsening of the Al_2CuMg precipitates. However, the coarsening process was only investigated qualitatively and no quantitative parameters of the S-phase were determined. The influence of creep experiments on the microstructural changes in alloy 2618A was studied qualitatively by Nový et al. [33,34]. They found that coarsening of the S-Phase occurs and denuded precipitate-free zones along the grain boundaries form after ageing at a temperature of 270 °C and different tensile loads. It is stated that these zones have a detrimental influence on the mechanical properties of the alloy. Based on this background, the present study aims to contribute to a more quantitative understanding of the S-phase coarsening process in alloy 2618A, especially regarding lower temperatures (≤ 200 °C) which are more relevant for operating conditions in engine applications. The quantitative comparison of the coarsening for isothermally aged samples with and without creep load allows determining if significant differences in the coarsening process under these two conditions occur. Possible differences have to be taken into account for lifetime prediction concepts of alloy 2618A.

2. Material and methods

The starting material for all fabricated and investigated samples are forged circular blanks made from alloy 2618A in T61 condition according to DIN EN 515 [35] with a chemical composition corresponding to DIN EN 573 shown in Table 1 [36]. The T61 condition is a heat treatment which includes a solution heat treatment and an additional heat treatment which leads to a slightly underaged condition. In this case the solution heat treatment was carried out at 530 °C for 8 h, followed by a quench in boiling water and ageing at 195 °C for 28 h. This temperature corresponds approximately to operation conditions and the temperature for the investigated samples.

Three square (3 cm \times 3 cm) bulk samples (thickness 4 mm) were cut by wire-cut electrical discharge machining from the blank for conventional ageing (without stress). The resulting cuboids were aged at 190 °C for 250 h, 2500 h, and 5000 h. Cylinders ($d = 3.7$ mm, $h = 6.2$ mm) were cut from the cuboids for the determination of the mechanical properties of material aged without stress. To determine the mechanical properties compression tests were performed on cylinders cut from the cuboids. The compressive proof strength was measured at 1% offset, $R_{p0.01}$, using the cylinders with two tests for each condition. In addition, cylindrical creep samples were machined with a gauge length

diameter of 6 mm from the blank orthogonal to the forging direction. These samples were subjected to creep testing at 190 °C with a stress of 181 MPa for 88.6 h and 400 h, a stress of 128 MPa for 1002 and 1820 h, and a stress of 79 MPa for 4172 h in a creep testing rig. The sample stressed at 181 MPa for 400 h broke during testing. The other samples remained intact until interruption of the creep test. However, it was necessary to decrease the sample stress for creep durations longer than 400 h to prevent breaking of the samples. The experimental conditions for the different samples and the results of the compression tests are shown in Table 2. The temperature accuracy of both heat treatments is ± 2 °C. The Brinell hardness HBW 2.5/62.5 was measured for all samples (see Table 2) to check if sample degradation took place. The hardness was determined from square (3 cm \times 3 cm) bulk samples (thickness 4 mm) using an Emco Test M4C 025 G3 hardness tester according to DIN EN 6506-1 for the stress-free aged samples (5 measurements, distances between sample edge and indentations ≥ 3 mm, and between indentations ≥ 3.5 mm) [37]. To acquire the hardness for the creep samples, the samples were cut in longitudinal direction and the first undeformed position nearest to the center of the creep samples was used for the measurement, thus perpendicular to the loading axis. An exception was made for Sample 5. A large amount of material from both sides of the creep sample center was needed to produce a suitable TEM sample and the hardness test had to be performed further away from the center of the specimen. The measurement uncertainty is ≤ 2.5 HBW for all samples. Subsequently, the samples were conventionally prepared for transmission electron microscopy. Platelets/discs were mechanically cut from the aged/creep tested samples with a thickness of about 500 μm . The discs were cut orthogonal to the loading direction. Then the samples were carefully ground using increasingly fine abrasive papers (down to grid size P1000) to a final thickness of about 130 μm . The final step of mechanical preparation was punching uniform discs with a diameter of 3 mm. To achieve electron transparency, the discs were electropolished by twin-jet polishing in a Tenupol-3 electropolishing device (Struers) at a voltage of 12 V. An electrolyte with two parts methanol (pure) and one part nitric acid (65%) cooled to -20 °C was used. The parameters for electropolishing were found without difficulties, since a thorough investigation by Ünlü is available [38].

The electron microscopical investigations were performed in a JEM-2200FS TEM/Scanning TEM transmission electron microscope with a field-emission gun operating at 200 kV. At least 15 images were taken at different places of each sample and at least 300 precipitates were evaluated for each presented radii distribution.

3. Experimental results

To systematically investigate the Al_2CuMg precipitate radii, dark-field transmission electron microscopy (DFTEM) was performed for all investigated samples. This allows selective imaging of the S-Phase precipitates and GPB-zones. The S-phase precipitates form as rods along the $\langle 001 \rangle_\alpha$ direction of the α -Al matrix. The GPB-zones as predecessors of the S-phase are also oriented along this direction. Therefore, the samples were oriented in the $[001]_\alpha$ direction for the DFTEM investigations.

Fig. 1 shows a selected area diffraction pattern of the investigated sample area with clearly visible reflections of the oriented Al-matrix exemplary for all samples. The rod shaped precipitates cause the streaks in between the matrix reflections [39]. An aperture was used to select the streaks for imaging as indicated by the circle. The insertion of the

Table 1
Nominal composition of alloy 2618A according to DIN EN 573.

Element	Cu	Mg	Fe	Ni	Si	Mn	Zn	Ti	Ti + Zr
Wt%	1.8–2.7	1.2–1.8	0.9–1.4	0.8–1.4	0.15–0.25	≤ 0.25	≤ 0.15	≤ 0.2	≤ 0.25

Download English Version:

<https://daneshyari.com/en/article/7973451>

Download Persian Version:

<https://daneshyari.com/article/7973451>

[Daneshyari.com](https://daneshyari.com)